HHS Public Access

Author manuscript

Brain Imaging Behav. Author manuscript; available in PMC 2023 February 01.

Published in final edited form as:

Brain Imaging Behav. 2022 February ; 16(1): 43–53. doi:10.1007/s11682-021-00475-y.

Effect of chemotherapy on default mode network connectivity in older women with breast cancer

Bihong T. Chen[a,b,*], **Zikuan Chen**[a], **Sunita K. Patel**[c], **Russell C. Rockne**[d], **Chi Wah Wong**[e], **James C. Root**[f], **Andrew J. Saykin**[g], **Tim A. Ahles**[f], **Andrei I. Holodny**[h], **Can-Lan Sun**[b], **Mina S. Sedrak**[i], **Heeyoung Kim**[b], **Ashley Celis**[b], **Vani Katheria**[b], **William Dale**[b,j]

[a]Department of Diagnostic Radiology, City of Hope National Medical Center, Duarte, CA 91010, United States

[b]Center for Cancer and Aging, City of Hope National Medical Center, Duarte, CA 91010, United States

[c]Department of Population Science, City of Hope National Medical Center, Duarte, CA 91010, United States

[d]Division of Mathematical Oncology, City of Hope National Medical Center, Duarte, CA 91010, United States

[e]Applied AI and Data Science, City of Hope National Medical Center, Duarte, CA 91010, United States

[f]Neurocognitive Research Lab, Memorial Sloan Kettering Cancer Center, New York, NY, United States

[g]Center for Neuroimaging, Indiana University School of Medicine, Indianapolis, IN, United States

[h]Department of Radiology, Memorial Sloan-Kettering Cancer Center, New York, NY, United States

[i]Department of Medical Oncology, City of Hope National Medical Center, Duarte, CA 91010, United States

[j]Department of Supportive Care Medicine, City of Hope National Medical Center, Duarte, CA 91010, United States

[*]**Corresponding author:** Bihong T. Chen, Department of Diagnostic Radiology, City of Hope National Medical Center, 1500 East Duarte Road, Duarte, CA 91010, Phone: +1 626 218 2318 Fax: +1 626 930 5451, Bechen@coh.org.

Authors' contributions:
Study design: BC, SP, AS, TA, WD
Manuscript preparation: BC, ZC, WD
Data analysis: BC, ZC, SP, CLS, HK, VK, WD
Interpretation and description of data: all authors
Statistical analysis: HK and CLS performed statistical analysis for the demographic data and the neuropsychological testing scores. ZC performed statistical analysis for the rs-fMRI data and correlation between rs-fMRI data and the neuropsychological testing scores.
Manuscript review and approval: All authors.

Conflicts of interest/Competing interests: All authors declare that they have no conflict of interests or competing interests.

Ethics approval: All procedures involving human participants were performed in accordance with the ethical standards of the Institutional Review Board of City of Hope and with the 1964 Helsinki Declaration and its later amendments, as well as with all local, state, and federal regulations.
This study is registered on Clinicaltrials.gov (NCT01992432).

Availability of data and material: The data and material will be provided to qualified researchers upon reasonable request.

Code availability: Code will be provided to qualified researchers upon reasonable request.

Abstract

Chemotherapy may impair cognition and contribute to accelerated aging. The purpose of this study was to assess the effects of chemotherapy on the connectivity of the default mode network (DMN) in older women with breast cancer. This prospective longitudinal study enrolled women aged ≥60 years with stage I–III breast cancer (CTx group) and matched healthy controls (HC group). Study assessments, consisting of resting-state functional MRI (rs-fMRI) and the Picture Sequence Memory (psm) test for episodic memory from the NIH Toolbox for Cognition, were obtained at baseline and within one month after the completion of chemotherapy for the CTx group and at matched intervals for the HC group. Two-sample t-test and FDR multiple comparison were used for statistical inference. Our analysis of the CTx group (N=19; 60–82 years of age, mean=66.6, SD=5.24) compared to the HC group (N=14; 60–78 years of age, mean=68.1, SD=5.69) revealed weaker DMN subnetwork connectivity in the anterior brain but stronger connectivity in the posterior brain at baseline. After chemotherapy, this pattern was reversed, with stronger anterior connectivity and weaker posterior connectivity. In addition, the meta-level functional network connectivity (FNC) among DMN subnetworks after chemotherapy was consistently weaker than the baseline FNC as seen in the couplings between anterior cingulate cortex (ACC) and retrosplenial (rSplenia) region, with ΔFNC('ACC','rSplenia')=−0.14, t value=−2.44, 95%CI=[−0.27, −0.10], $p_{FDR}<0.05$). The baseline FNC matrices of DMN subnetworks were correlated with psm scores (corr=0.58, $p<0.05$). Our results support DMN alterations as a potential neuroimaging biomarker for cancer-related cognitive impairment and accelerated aging.

Keywords

cancer-related cognitive impairment (CRCI); breast cancer; chemotherapy; episodic memory; default mode network

Introduction

Cancer patients undergoing anti-cancer treatment frequently experience cancer-related cognitive impairment (CRCI) (T. A. Ahles & J. C. Root, 2018; Ahles & Saykin, 2007). Neuropsychological studies have reported CRCI in up to 70% of patients receiving chemotherapy, primarily affecting their memory, processing speed, and executive function (Wefel, Vardy, Ahles, & Schagen, 2011). As cancer, chemotherapy, and aging process affect overlapping neurobiological systems, exposure to chemotherapy can also alter or accelerate the aging process, particularly in older cancer patients, which may further jeopardize their quality of life, and cognition (Mandelblatt et al., 2018; Nguyen & Ehrlich, 2020). Thus, assessing the potential association between cancer treatment and aging will aid in the development of interventions to prevent and mitigate the adverse effects of cancer and treatment on cognitive functioning (Guida et al., 2020).

DMN consists of highly interconnected neocortical regions, typically including the posterior cingulate cortex (PCC), precuneus, anterior cingulate cortex (ACC), and medial prefrontal cortex (mPFC) (Damoiseaux et al., 2006; Raichle et al., 2001). It plays an important role in implicit learning, introspective and reflective self-awareness processes, and episodic

memory retrieval (Y. Chen et al., 2019). Functional connectivity (FC) analyzes the temporal correlations between spatially separated brain regions, which helps to assess how brain regions interact to support cognitive function (Dumas et al., 2013). Alterations to the default mode network (DMN) have been observed in breast cancer patients after chemotherapy, and DMN may, in fact, be more vulnerable to chemotherapy than other brain networks (Dumas et al., 2013; Hosseini & Kesler, 2014; Kesler, 2014; Kesler et al., 2013; Miao et al., 2016). Kesler et al. found that breast cancer survivors with chemotherapy could be distinguished from survivors without chemotherapy and healthy controls based on a multivariate analysis of their DMN connectivity (Kesler et al., 2013). In addition, Bruno et al. found that, compared to healthy controls, breast cancer survivors treated with chemotherapy displayed altered topological organization of the global brain network and disrupted regional network characteristics in the frontal, temporal, and striatal regions (Bruno, Hosseini, & Kesler, 2012). However, none of the prior studies has focused on older adults who represent almost half of the new breast cancer cases in the United States (Hayat, Howlader, Reichman, & Edwards, 2007). There is limited information on brain connectivity and DMN alterations in older patients receiving chemotherapy. Furthermore, even less is known about the trajectory of connectivity changes over time in the older chemotherapy-treated patients due to lack of longitudinal studies, presenting a gap in knowledge in our understanding of neural correlates for CRCI in the aging population.

Episodic memory has been shown to be impacted by cancer and chemotherapy leading to CRCI (Tim A. Ahles & James C. Root, 2018; Pergolizzi et al., 2019). In addition, episodic memory is also considered as the hallmark of aging as it is the most age sensitive measure among all human memory system and there are brain changes associated with age-related episodic memory decline (Nyberg & Pudas, 2019). Furthermore, episodic memory and DMN reflect similar brain function as longitudinal DMN alterations are correlated with changes in episodic memory in healthy older adults (Qi et al., 2010; Staffaroni et al., 2018). Disruption of DMN connectivity is a promising neuroimaging biomarker for both aging and disease-related cognitive decline (Damoiseaux, 2012, 2017; Dennis & Thompson, 2014). This notion has been further supported by Pergolizzi et al. who showed a posterior-anterior shift of neural processing during a visual episodic memory task in breast cancer patients following chemotherapy, which was consistent with accelerated aging (Pergolizzi et al., 2019). Therefore, episodic memory should be one of the most relevant cognitive testing measures in assessing DMN connectivity in older patients with cancer.

Here, we report a prospective longitudinal study of brain connectivity focusing on older women with breast cancer. We aimed to assess DMN connectivity alterations through comprehensive analysis of resting-state functional MRI (rs-fMRI) data and to explore the potential association between DMN and episodic memory in older breast cancer patients undergoing chemotherapy. Specifically, using a seed-based approach, we constructed FC maps and assessed alterations in a collection of 12 seed-initiated DMN subnetworks. Then, we proceeded to construct a DMN functional network connectivity (FNC) matrix for a meta-level graph theoretical analysis among the 12 seed-initiated DMN subnetworks. In addition, we explored the correlation between the DMN FNC and the neuropsychological testing scores for episodic memory. We hypothesized that DMN connectivity would differ

between older women with breast cancer and healthy controls at baseline, would be altered following chemotherapy, and FNC alterations would be correlated with episodic memory.

Methods

Study design:

This study enrolled women aged ≥60 years with stage I–III breast cancer prior to adjuvant chemotherapy (CTx group). Age matched females without a history of cancer were enrolled as healthy controls (HC group). The CTx group and the HC group were matched by age and sex. Eligibility criteria included women at age ≥ 60 years with a diagnosis of stage I–III breast cancer who had no history of psychiatric disease, neurodegenerative disorders, stroke or other cancer diagnosis. HCs were recruited with the same eligibility criteria, excluding the cancer diagnosis. Participants with a history of neurological, psychiatric or cerebrovascular disorders such as stroke were excluded.

A pre-chemotherapy baseline assessment (time point 1, TP1), including rs-fMRI scan and the National Institutes of Health (NIH) Toolbox Cognition Battery (Gershon et al., 2013; Weintraub et al., 2013) was conducted after breast surgery and before the initiation of chemotherapy. A follow-up assessment (time point 2, TP2) was conducted within one month after the last chemotherapy infusion. The same assessments were obtained at matched intervals for the HC group. The participants' clinical data, such as age, race, cancer staging, and chemotherapy regimen, were obtained from medical records. Written informed consent was obtained from all study participants. The research protocol was approved by the Institutional Review Board at City of Hope National Medical Center.

Brain rs-fMRI data acquisition:

Brain rs-fMRI has been recommended by the International Cognition and Cancer Task Force (ICCTF) as a minimal requirement for CRCI neuroimaging research (Deprez et al., 2018). Our rs-fMRI data was obtained using the same 3T Verio Siemens scanner (Siemens, Erlangen, Germany) with a 12-channel head coil, as reported in detail elsewhere (B. T. Chen, T. Jin, et al., 2019). Brain rs-fMRI data was acquired using rapid gradient echo-planar pulse imaging (EPI) with the following parameters: TR/TE=2000/25 millisecond, flip angle=80°, voxel=3.5×3.5×3.5 mm^3, matrix=64×64×32, total volume number=160, and total acquisition time=5.4 minutes. During scanning, the participants were instructed to keep their eyes closed without thinking about anything or falling asleep.

Neuropsychological testing:

Picture Sequence Memory (psm) test for episodic memory from the NIH Toolbox Cognition Battery (Gershon et al., 2013; Weintraub et al., 2013) was assessed for all participants at both TP1 and TP2. The psm test was a measure of episodic memory involving the acquisition, storage and effortful recall of new information (Gershon et al., 2013; Weintraub et al., 2013). Testing was performed in a quiet area outside of the MRI scanner.

Preprocessing of brain 4D rs-fMRI data:

Each raw fMRI dataset consisted of a spatiotemporal time series of volumes in a 4D array (64×64×32×160). Each dataset underwent standard processing with Statistical Parametric Mapping version 12 (SPM 12), including time series image realignment, slice timing, spatial normalization to the Montreal Neurological Institute (MNI) standard brain space with resampling in 3×3×3 mm^3 voxels, and spatial smoothing with a Gaussian kernel of FWHM (full-width at half-max)=6 mm (≤2 voxels) (Z. Chen & Calhoun, 2018). We performed the standard SPM processing, which included the 'realignment' and 'slice timing' procedures. The first four time points were removed from the time series data to avoid using the potentially unstable data during the initial data collection. After preprocessing, each subject-specific fMRI dataset was represented by a 4D array in size of 53×63×46×156.

DMN seed regions and subnetworks:

FC was assessed using a seed-based approach in which a "seed" region of interest was selected and a time series of voxel signals at the seed were extracted (Fox & Raichle, 2007). The time course of voxel signals was temporally filtered at a pass band [0.01,0.1] Hz to retain the slow homodynamic activity, and to decrease the physiological noise and very low-frequency drift. For each seed voxel, we calculated a whole-brain FC map by functional correlations, which was considered a seed-initiated DMN subnetwork.

Brain regions with strong positive correlations in connectivity were considered functionally coupled, regardless of their spatial separation (Dennis & Thompson, 2014). We obtained a collection of 12 DMN subnetworks from the 12 seeds (Fig. 1, Supplemental Table 1). Each subject-specific DMN system was comprised of all 12 DMN subnetworks.

FNC matrices:

The interconnections among the DMN subnetworks were assessed based on a graph theory analysis (Barnett, Buckley, & Bullock, 2011; V. C. Chen, Lin, Tsai, & Weng, 2020; Sporns, 2012). Specifically, relationships between the time series of 12 seeds were analyzed in a 12×12 connectivity matrix for each participant's dataset, which was considered as a meta-level analysis over the 12 FC subnetworks and was termed a functional network connectivity (FNC). A FNC matrix (Fig. 1) was constructed by considering each of the 12 seed-initiated subnetworks in a participant's DMN system as a node and by calculating the edges reflective of the temporal correlations among the 12 nodes.

Correlations between FNC matrix and psm testing scores:

A 12×12 psm-FNC correlation matrices were constructed using subject-specific psm scores (e.g., a vector of 19 scores for the CTx group) and subject-specific FNC matrices (e.g., a 12×12×19 matrix for the CTx group) for both the CTx and the HC groups. Similar correlation matrices were constructed using various paired combinations among psm, FNC, Δpsm, and ΔFNC.

Statistical analysis:

In summary, we performed statistical data analysis on both the CTx group and the HC group for both TP1 and TP2 on the demographic information, DMN subnetworks (FC maps), and DMN FNC matrices, and neuropsychological testing scores (psm scores). We applied paired two-sample t-tests for longitudinal changes and the unpaired two-sample t-tests for between group differences (including baseline differences and group-by-time interactions). We conducted False Discovery Rate (FDR) multiple comparisons for statistical inference (significance at $p_{FDR}<0.05$). All statistical analyses were implemented in MATLAB statistical toolbox.

Specifically, the demographic data were compared between the CTx group and the HC groups with two-sample t-test and chi-square test. The longitudinal changes in FNC matrices for within-group differences from TP1 to TP2 were performed with paired two-sample t-tests. The statistical *p*-value matrices were used to assess statistical robustness by multiple comparisons. Two-sampled unpaired t-tests were used for between-group comparisons, and the resultant *p*-values were used to assess statistical significance. FDR method was used for multiple comparisons, with statistical significance set to $p_{\text{FDR corrected}}<0.05$ (Benjamini & Hochberg, 1995). To examine differences in ΔFNC between the CTx and HC groups for group-by-time interaction for a 12×12 symmetrical *p*-value matrix, correction for multiple comparisons was applied to a set of 66 simultaneous variables [12×(12−1)/2 or half of the element numbers in a symmetrical 12×12 matrix].

A correlation analysis was conducted between the FNC couplings and the psm scores. After obtaining psm-correlated FNC matrices and corresponding *p*-value matrices in the size of 12×12, the following statistical analyses were performed: 1) individual *p*-value thresholding of each element at $p<0.05$; and 2) FDR correction for multiple comparisons ($p_{FDR}<0.05$). This procedure was also performed for the psm-correlated ΔFNC analysis.

Results

Study participants:

Detailed demographic information for this cohort has been reported in our prior studies (B. T. Chen et al., 2018; B. T. Chen, N. Ye, et al., 2019). However, we have not previously assessed DMN for this cohort. In addition, there were differences in the number of patients between this study and our previous reports (B. T. Chen et al., 2018; B. T. Chen, N. Ye, et al., 2019). For example, since publishing the gray matter density data (B. T. Chen et al., 2018), we have completed assessments for three additional patients (two at Stage I and one at Stage II breast cancer). Briefly, the current study enrolled 33 participants, 19 patients in the CTx group (60–82 years of age) and 14 in the HC group (60–78 years of age)(B. T. Chen, N. Ye, et al., 2019). There were no significant baseline differences between the two groups in age or education ($p>0.05$) (Table 1). The chemotherapy regimens and sessions were varied among the patients.

Baseline DMN subnetworks:

For the CTx group, there were distinct functional blobs indicating the seed regions and the regions with which a strong functional connectivity was shared with $corr_{DMN}>0.90$ (Fig. 2a). The DMN display threshold was empirically specified at 0.90 to display the functional connectivity blobs. Some DMN subnetwork was comprised of a single blob such as the medial prefrontal cortex ('mPFC') subnetwork, indicating no remote (or far) connectivity with other brain regions.

We detected baseline differences in DMN subnetworks between the CTx group and the HC group, using $|\Delta corr|>0.15$ (Fig. 2b and Fig. 2c). The threshold of 0.15 was empirically specified to display the large baseline differences while suppressing the small differences. The CTx group showed weaker connectivity initiated from 'mPFC', 'R Front: right frontal lobe', 'R Temp: right temporal lobe', 'L Hippo: left hippocampus' and 'R Hippo: right hippocampus', and stronger connectivity initiated from 'L Pariet: left parietal lobe' and 'R Pariet: right parietal lobe'. Notably, in the 'ACC: anterior cingulate cortex' subnetwork, the CTx group showed stronger connectivity to the posterior region than the HC group but weaker connectivity to the anterior region at baseline (in Fig. 2c).

Longitudinal changes of DMN subnetwork:

We estimated longitudinal changes of DMN FC subnetworks from TP1 to TP2 (ΔDMN) for the CTx group, which was displayed with an empirical thresholding of $\Delta corr>0.15$ (Fig. 3a). For the CTx group, we observed increased connectivity in subnetworks of 'L Front', 'R Front' and 'R Temp', and decreased connectivity in subnetworks of 'mPFC', 'L Temp', and 'rSplenia: retrosplenial'. In the 'ACC' subnetwork, we observed increased connectivity to the anterior region and decreased connectivity to the posterior region.

A group-by-time interaction analysis indicated that DMN FC subnetworks in the CTx group were significantly more diminished from TP1 to TP2 (Fig. 3b) compared to those in the HC group as shown in Fig 3b (displayed by a thresholding $\Delta corr>0.15$). This effect was most predominant in subnetworks of 'ACC', 'L Parietal', and 'rSplenia'.

Meta-level FNC matrices:

Using the subject-specific DMN subnetworks as presented in the FC maps, we rendered a meta-level analysis in a FNC matrix in the size of 12×12 for the12 DMN subnetworks. When comparing baseline FNC couplings in the CTx and HC groups, we observed four statistically significant FNC couplings with $p_{FDR}<0.05$ (Table 2). The CTx group showed two stronger FNC couplings between 'ACC' and 'L Temp' and between 'ACC' and 'rSplenia', and two weaker couplings between 'R Temp' and 'R Hippo' and between 'L Hippo' and 'rSplenia'.

When assessing the longitudinal changes in FNC from TP1 to TP2 (ΔFNC) in the CTx group (Fig. 1c, Table 2), we observed six FNC couplings, all showing reduced connectivity ($p_{FDR}<0.05$) such as couplings between 'mPFC' and 'L Temp', and between 'ACC' and 'rSplenia'.

A group-by-time interaction analysis revealed eight FNC couplings with negative interactions between the CTx group and the HC group ($p_{FDR}<0.05$), indicating that a FNC decrease from TP1 to TP2 for the CTx group was always related to a FNC increase for the HC group, and vice versa (Table 2, Supplemental Fig. 1). The most significant difference between the longitudinal FNC changes for the two groups was observed between 'mPFC' and 'L Front'. The FNC changes were negative for the CTx group but positive for the HC group, with a difference in magnitude of 0.20, indicating a significant group-by-time interaction in the anterior brain.

Correlation between FNC matrices and psm scores:

We found no significant between-group differences in psm scores at TP1 (p=0.10) or at TP2 (p=0.98) (Table 1) nor significant within-group differences from TP1 to TP2 for the CTx group (p=0.60) or for the HC group (p=0.44). In addition, there were no statistically significant group-by-time interactions (p=0.10).

Correlative analysis between psm scores and FNC matrices identified statistically significant elementwise correlations using $p<0.05$ (Supplemental Fig. 2). For the CTx group at baseline, we identified two FNC couplings, i.e., between 'L Front' and 'R Temp' (corr=0.53) and between 'L Front' and 'R Hippo' (corr=0.58), as being significantly correlated with psm scores. Of note, there were no significant correlations between baseline psm score and ΔFNC, baseline FNC and Δpsm, or ΔFNC and Δpsm in either group.

Discussion

In this study, we observed weaker anterior and stronger posterior DMN connectivity at baseline prior to chemotherapy in the CTx group compared with the HC group; following chemotherapy, this pattern was reversed, indicating a chemotherapy-associated posterior-anterior shift. In addition, we found consistently weaker meta-level FNC following chemotherapy in mostly posterior-anterior couplings between the posterior seeds in the retrosplenial/parietal regions and the anterior seeds in the frontal/temporal lobes. Furthermore, we identified two FNC couplings between left frontal lobe and right temporal lobe and between left frontal lobe and right hippocampus being significantly correlated with the psm scores for episodic memory in the CTx group prior to chemotherapy treatment. To the best of our knowledge, this was the first prospective longitudinal study focusing on older women with breast cancer for assessing the acute effects of chemotherapy on large-scale brain functional networks. Our study contributed pilot data supporting DMN connectivity alterations as neuroimaging biomarkers of cognitive function for older patients with cancer undergoing chemotherapy.

Our findings of reduced DMN connectivity following chemotherapy were generally in line with prior reports in younger cohorts (Kesler, 2014; Kesler et al., 2013). For example, we found decreased connectivity in the posterior brain of our older patients after chemotherapy, similar to the prior report of reduced connectivity in the precuneus which was a posterior brain region, in patients with breast cancer after chemotherapy (Dumas et al., 2013). However, we observed more extensive DMN alterations involving additional brain regions. In addition, we found specific FNC couplings with altered connectivity including the

anterior-posterior coupling between the anterior brain such as the anterior cingulate gyrus and the frontal lobe and the posterior brain such as retrosplenial and parietal lobe. These findings of connectivity changes may be unique for older cancer patients, providing support for DMN alterations as a potential neuroimaging biomarker of CRCI in older adults receiving chemotherapy.

Our results also showed an association between DMN and accelerated aging in chemotherapy-treated older cancer patients. Specifically, we observed a posterior-anterior shift of DMN connectivity following chemotherapy, suggesting the occurrence of accelerated aging, which was consistent with published literature on CRCI (Pergolizzi et al., 2019). Previously, Pergolizzi et al. assessed patterns of neural activity associated with an episodic memory task in breast cancer patients and showed a posterior-anterior shift in brain activity following chemotherapy (Pergolizzi et al., 2019). They attributed this shift in brain activity and accelerated aging to the compensatory activation of the anterior brain in response to the visual processing deficiencies in the posterior brain. Although our study differed in being focused on older adults receiving chemotherapy for breast cancer and analyzed resting-state brain connectivity rather than task-related activity as in their study, a similar compensatory mechanism might be responsible for our observation of posterior-anterior shift as seen in cancer and aging research (Qi et al., 2010; Staffaroni et al., 2018). The posterior-anterior shift in aging represents a general phenomenon of brain aging, which is characterized by age-related reductions in occipital activity but increases in frontal activity (McCarthy, Benuskova, & Franz, 2014; Pergolizzi et al., 2019). Our observation of the posterior-anterior shift appeared to be accentuated by chemotherapy as it was specific for the CTx group and not seen in the HCs. This finding was significant as it implicated accelerated aging in the chemotherapy-treated older patients, which may help to understand cognitive impairment in older cancer survivors.

Patients being treated for cancer may suffer accelerated aging that causes steeper declines in cognitive function compared to non-cancer populations (Ahles & Hurria, 2018; Guida et al., 2019; Mandelblatt et al., 2016; Mandelblatt et al., 2013; Margolick & Ferrucci, 2015). However, the underlying biological mechanisms are not fully understood. Nevertheless, brain structural changes correlated with CRCI have been noted. Our own data showed significantly greater longitudinal reductions in gray matter density in DMN regions, such as the left anterior cingulate gyrus, right insula, and left middle temporal gyrus, in older patients following chemotherapy, compared to healthy controls (B. T. Chen et al., 2018). We also found white matter microstructural changes following chemotherapy in the corpus callosum and the left superior longitudinal fasciculus connecting anterior (frontal lobe) to posterior (parietal lobe) brain (B. T. Chen, N. Ye, et al., 2019), as well as altered intrinsic brain activity in right anterior cingulate gyrus and left precuneus (B. T. Chen, T. Jin, et al., 2019). Thus, converging evidence indicates a brain structural basis for functional alterations underlying CRCI in older patients with cancer receiving chemotherapy. We speculate that brain structure and the DMN connectivity are closely related to maintain cognitive function of older adults undergoing cancer treatment.

Our study also indicated that pre-treatment DMN connectivity was different in the CTx group compared to the HC group, consistent with work by others (Bruno et al., 2012; Dumas

et al., 2013; Kesler et al., 2013; Miao et al., 2016).Kesler et al. reported that specific pre-treatment altered local connectivity in specific brain regions--such as right middle inferior orbital frontal gyrus, right medial superior frontal gyrus and right inferior parietal lobe--may predict long-term cognitive outcomes following breast cancer (Kesler et al., 2017). Interestingly, we also found significant pre-treatment correlations between functional couplings and neurocognitive testing scores unique to the CTx group. We hypothesize that these pre-treatment functional alterations were related to CRCI. Further work is needed to elucidate the pre-treatment alterations.

There were several limitations. First, this single-center study with a small sample size included a group of patients with different cancer stages and chemotherapy regimens, which may have contributed to the variability in DMN connectivity. Our small sample size may also be partly responsible for the lack of significant findings in the cognitive testing scores and for lack of significant correlations between DMN alterations and cognitive scores. Similar limitations have been reported by others (McDonald, Conroy, Smith, West, & Saykin, 2013), indicating a need for larger cohorts through multi-center collaborations, such as the on-going ICCTF neuroimaging data-pooling approach. Additionally, our small sample size lacked the statistical power to assess DMN connectivity according to chemotherapy regimen or to evaluate the correlation between the DMN alterations and disease progression or severity. Second, our study, while including healthy controls, did not have a matched group of breast cancer patients without chemotherapy, so we could not tease out the effects of cancer on DMN connectivity or cognition. Third, we selectively assessed episodic memory using the psm test rather than a comprehensive neuropsychological testing battery. We selected episodic memory test because of its close association with brain changes in chemotherapy-treated patients (Pergolizzi et al., 2019) and also because of its sensitivity to age-related changes (Damoiseaux, 2012, 2017; Dennis & Thompson, 2014), which was important for our study on older patients with cancer undergoing chemotherapy. Finally, without long-term follow-up assessment, we were not able to assess the potential recovery of DMN alterations following chemotherapy. Future studies will be necessary to understand the trajectory of accelerated aging and to detect the critical time when the chemotherapy-associated brain alterations diverge from normal aging.

Conclusion

The results from this pilot study suggested close association among DMN alterations, cognitive function and aging in the older adults with cancer. We observed a posterior-anterior shift of DMN connectivity in older patients treated with chemotherapy, implicating chemotherapy-associated accelerated aging. We also found consistently weaker meta-level FNC with altered functional couplings after chemotherapy, which may be unique for older cancer patients. Future studies with larger sample size and long-term follow up are necessary to validate our results and to explore the DMN alterations as potential neuroimaging biomarkers for CRCI. This is important as biomarkers may help to detect and offer targets to mitigate the adverse effects of treatment on cognition for older adults with cancer undergoing chemotherapy.

Supplementary Material

Refer to Web version on PubMed Central for supplementary material.

Acknowledgments

Preliminary data was presented as a poster at the International Cognition and Cancer Task Force (ICCTF) conference in Denver, CO, USA. Feb. 3-5, 2020.

Kerin Higa, PhD, provided editing assistance.

Funding:

This study was funded by National Institutes of Health/National Institute on Aging grants R03 AG045090-02 (BC) and K24 AG055693-01 (WD). BTC received funding support from the City of Hope Center for Cancer and Aging.

References

Ahles TA, & Hurria A (2018). New Challenges in Psycho-Oncology Research IV: Cognition and cancer: Conceptual and methodological issues and future directions. Psycho-Oncology, 27(1), 3–9. doi:10.1002/pon.4564

Ahles TA, & Root JC (2018). Cognitive Effects of Cancer and Cancer Treatments. Annual Review of Clinical Psychology, 14, 425–451. doi:10.1146/annurev-clinpsy-050817-084903

Ahles TA, & Root JC (2018). Cognitive Effects of Cancer and Cancer Treatments. Annual Review of Clinical Psychology, 14(1), 425–451. doi:10.1146/annurev-clinpsy-050817-084903

Ahles TA, & Saykin AJ (2007). Candidate mechanisms for chemotherapy-induced cognitive changes. Nature Reviews Cancer, 7(3), 192–201. doi:10.1038/nrc2073 [PubMed: 17318212]

Barnett L, Buckley CL, & Bullock S (2011). Neural complexity: a graph theoretic interpretation. Physical Review. E: Statistical, Nonlinear, and Soft Matter Physics, 83(4 Pt 1), 041906. doi:10.1103/PhysRevE.83.041906

Benjamini Y, & Hochberg Y (1995). Controlling the false discovery rate: A practical and powerful approach to multiple testing. Journal of the Royal Statistical Society, Series B (Methodological), 57(1), 269–300.

Bruno J, Hosseini SM, & Kesler S (2012). Altered resting state functional brain network topology in chemotherapy-treated breast cancer survivors. Neurobiol Dis, 48(3), 329–338. doi:10.1016/j.nbd.2012.07.009 [PubMed: 22820143]

Chen BT, Jin T, Patel SK, Ye N, Ma H, Wong CW, … Dale W (2019). Intrinsic brain activity changes associated with adjuvant chemotherapy in older women with breast cancer: a pilot longitudinal study. Breast Cancer Research and Treatment, 176(1), 181–189. doi:10.1007/s10549-019-05230-y [PubMed: 30989462]

Chen BT, Jin T, Patel SK, Ye N, Sun CL, Ma H, … Hurria A (2018). Gray matter density reduction associated with adjuvant chemotherapy in older women with breast cancer. Breast Cancer Research and Treatment, 172(2), 363–370. doi:10.1007/s10549-018-4911-y [PubMed: 30088178]

Chen BT, Ye N, Wong CW, Patel SK, Jin T, Sun CL, … Dale W (2019). Effects of chemotherapy on aging white matter microstructure: A longitudinal diffusion tensor imaging study. Journal of Geriatric Oncology. doi:10.1016/j.jgo.2019.09.016

Chen VC, Lin KY, Tsai YH, & Weng JC (2020). Connectome analysis of brain functional network alterations in breast cancer survivors with and without chemotherapy. PloS One, 15(5), e0232548. doi:10.1371/journal.pone.0232548 [PubMed: 32365133]

Chen Y, Ou Y, Lv D, Yang R, Li S, Jia C, … Li P (2019). Altered network homogeneity of the default-mode network in drug-naive obsessive-compulsive disorder. Progress in Neuro-Psychopharmacology and Biological Psychiatry, 93, 77–83. doi:10.1016/j.pnpbp.2019.03.008 [PubMed: 30905622]

Chen Z, & Calhoun V (2018). Effect of Spatial Smoothing on Task fMRI ICA and Functional Connectivity. Front Neurosci, 12, 15. doi:10.3389/fnins.2018.00015 [PubMed: 29456485]

Damoiseaux JS (2012). Resting-state fMRI as a biomarker for Alzheimer's disease? Alzheimer's Research & Therapy, 4(2), 8. doi:10.1186/alzrt106

Damoiseaux JS (2017). Effects of aging on functional and structural brain connectivity. Neuroimage, 160, 32–40. doi:10.1016/j.neuroimage.2017.01.077 [PubMed: 28159687]

Damoiseaux JS, Rombouts SA, Barkhof F, Scheltens P, Stam CJ, Smith SM, & Beckmann CF (2006). Consistent resting-state networks across healthy subjects. Proceedings of the National Academy of Sciences of the United States of America, 103(37), 13848–13853. doi:10.1073/pnas.0601417103 [PubMed: 16945915]

Dennis EL, & Thompson PM (2014). Functional brain connectivity using fMRI in aging and Alzheimer's disease. Neuropsychology Review, 24(1), 49–62. doi:10.1007/s11065-014-9249-6 [PubMed: 24562737]

Deprez S, Kesler SR, Saykin AJ, Silverman DHS, de Ruiter MB, & McDonald BC (2018). International Cognition and Cancer Task Force Recommendations for Neuroimaging Methods in the Study of Cognitive Impairment in Non-CNS Cancer Patients. Journal of the National Cancer Institute, 110(3), 223–231. doi:10.1093/jnci/djx285 [PubMed: 29365201]

Dumas JA, Makarewicz J, Schaubhut GJ, Devins R, Albert K, Dittus K, & Newhouse PA (2013). Chemotherapy altered brain functional connectivity in women with breast cancer: a pilot study. Brain Imaging Behav, 7(4), 524–532. doi:10.1007/s11682-013-9244-1 [PubMed: 23852814]

Fox MD, & Raichle ME (2007). Spontaneous fluctuations in brain activity observed with functional magnetic resonance imaging. Nature Reviews: Neuroscience, 8(9), 700–711. doi:10.1038/nrn2201 [PubMed: 17704812]

Gershon RC, Wagster MV, Hendrie HC, Fox NA, Cook KF, & Nowinski CJ (2013). NIH toolbox for assessment of neurological and behavioral function. Neurology, 80(11 Suppl 3), S2–6. doi:10.1212/WNL.0b013e3182872e5f [PubMed: 23479538]

Guida JL, Agurs-Collins T, Ahles TA, Campisi J, Dale W, Demark-Wahnefried W, … Ness KK (2020). Strategies to Prevent or Remediate Cancer and Treatment-Related Aging. Journal of the National Cancer Institute. doi:10.1093/jnci/djaa060

Guida JL, Ahles TA, Belsky D, Campisi J, Cohen HJ, DeGregori J, … Hurria A (2019). Measuring Aging and Identifying Aging Phenotypes in Cancer Survivors. Journal of the National Cancer Institute, 111(12), 1245–1254. doi:10.1093/jnci/djz136 [PubMed: 31321426]

Hayat MJ, Howlader N, Reichman ME, & Edwards BK (2007). Cancer statistics, trends, and multiple primary cancer analyses from the Surveillance, Epidemiology, and End Results (SEER) Program. The Oncologist, 12(1), 20–37. doi:12/1/20 [pii] 10.1634/theoncologist.12-1-20. [PubMed: 17227898]

Hosseini SM, & Kesler SR (2014). Multivariate pattern analysis of FMRI in breast cancer survivors and healthy women. Journal of the International Neuropsychological Society, 20(4), 391–401. doi:10.1017/s1355617713001173 [PubMed: 24135221]

Kesler SR (2014). Default mode network as a potential biomarker of chemotherapy-related brain injury. Neurobiology of Aging, 35 Suppl 2, S11–19. doi:10.1016/j.neurobiolaging.2014.03.036 [PubMed: 24913897]

Kesler SR, Rao A, Blayney DW, Oakley-Girvan IA, Karuturi M, & Palesh O (2017). Predicting Long-Term Cognitive Outcome Following Breast Cancer with Pre-Treatment Resting State fMRI and Random Forest Machine Learning. Frontiers in Human Neuroscience, 11, 555. doi:10.3389/fnhum.2017.00555 [PubMed: 29187817]

Kesler SR, Wefel JS, Hosseini SM, Cheung M, Watson CL, & Hoeft F (2013). Default mode network connectivity distinguishes chemotherapy-treated breast cancer survivors from controls. Proceedings of the National Academy of Sciences of the United States of America, 110(28), 11600–11605. doi:10.1073/pnas.1214551110 [PubMed: 23798392]

Mandelblatt JS, Clapp JD, Luta G, Faul LA, Tallarico MD, McClendon TD, … Isaacs C (2016). Long-term trajectories of self-reported cognitive function in a cohort of older survivors of breast cancer: CALGB 369901 (Alliance). Cancer, 122(22), 3555–3563. doi:10.1002/cncr.30208 [PubMed: 27447359]

Mandelblatt JS, Hurria A, McDonald BC, Saykin AJ, Stern RA, VanMeter JW, … Living With Cancer, S. (2013). Cognitive effects of cancer and its treatments at the intersection of aging:

what do we know; what do we need to know? Seminars in Oncology, 40(6), 709–725. doi:10.1053/j.seminoncol.2013.09.006 [PubMed: 24331192]

Mandelblatt JS, Small BJ, Luta G, Hurria A, Jim H, McDonald BC, … Ahles T (2018). Cancer-Related Cognitive Outcomes Among Older Breast Cancer Survivors in the Thinking and Living With Cancer Study. Journal of Clinical Oncology, 36(32), Jco1800140. doi:10.1200/jco.18.00140

Margolick JB, & Ferrucci L (2015). Accelerating aging research: how can we measure the rate of biologic aging? Experimental Gerontology, 64, 78–80. doi:10.1016/j.exger.2015.02.009 [PubMed: 25683017]

McCarthy P, Benuskova L, & Franz EA (2014). The age-related posterior-anterior shift as revealed by voxelwise analysis of functional brain networks. Frontiers in Aging Neuroscience, 6, 301. doi:10.3389/fnagi.2014.00301 [PubMed: 25426065]

McDonald BC, Conroy SK, Smith DJ, West JD, & Saykin AJ (2013). Frontal gray matter reduction after breast cancer chemotherapy and association with executive symptoms: a replication and extension study. Brain, Behavior, and Immunity, 30 Suppl, S117–125. doi:10.1016/j.bbi.2012.05.007

Miao H, Chen X, Yan Y, He X, Hu S, Kong J, … Qiu B (2016). Functional connectivity change of brain default mode network in breast cancer patients after chemotherapy. Neuroradiology, 58(9), 921–928. doi:10.1007/s00234-016-1708-8 [PubMed: 27278455]

Nguyen LD, & Ehrlich BE (2020). Cellular mechanisms and treatments for chemobrain: insight from aging and neurodegenerative diseases. EMBO Molecular Medicine, 12(6), e12075. doi:10.15252/emmm.202012075 [PubMed: 32346964]

Nyberg L, & Pudas S (2019). Successful Memory Aging. 70(1), 219–243. doi:10.1146/annurev-psych-010418-103052

Pergolizzi D, Root JC, Pan H, Silbersweig D, Stern E, Passik SD, & Ahles TA (2019). Episodic memory for visual scenes suggests compensatory brain activity in breast cancer patients: a prospective longitudinal fMRI study. Brain Imaging and Behavior, 13(6), 1674–1688. doi:10.1007/s11682-019-00038-2 [PubMed: 30680610]

Qi Z, Wu X, Wang Z, Zhang N, Dong H, Yao L, & Li K (2010). Impairment and compensation coexist in amnestic MCI default mode network. Neuroimage, 50(1), 48–55. doi:10.1016/j.neuroimage.2009.12.025 [PubMed: 20006713]

Raichle ME, MacLeod AM, Snyder AZ, Powers WJ, Gusnard DA, & Shulman GL (2001). A default mode of brain function. Proceedings of the National Academy of Sciences of the United States of America, 98(2), 676–682. doi:10.1073/pnas.98.2.676 [PubMed: 11209064]

Sporns O (2012). From simple graphs to the connectome: networks in neuroimaging. Neuroimage, 62(2), 881–886. doi:10.1016/j.neuroimage.2011.08.085 [PubMed: 21964480]

Staffaroni AM, Brown JA, Casaletto KB, Elahi FM, Deng J, Neuhaus J, … Kramer JH (2018). The Longitudinal Trajectory of Default Mode Network Connectivity in Healthy Older Adults Varies As a Function of Age and Is Associated with Changes in Episodic Memory and Processing Speed. Journal of Neuroscience, 38(11), 2809–2817. doi:10.1523/jneurosci.3067-17.2018 [PubMed: 29440553]

Wefel JS, Vardy J, Ahles T, & Schagen SB (2011). International Cognition and Cancer Task Force recommendations to harmonise studies of cognitive function in patients with cancer. Lancet Oncology, 12(7), 703–708. doi:10.1016/s1470-2045(10)70294-1 [PubMed: 21354373]

Weintraub S, Dikmen SS, Heaton RK, Tulsky DS, Zelazo PD, Bauer PJ, … Gershon RC (2013). Cognition assessment using the NIH Toolbox. Neurology, 80(11 Supplement 3), S54–S64. doi:10.1212/WNL.0b013e3182872ded [PubMed: 23479546]

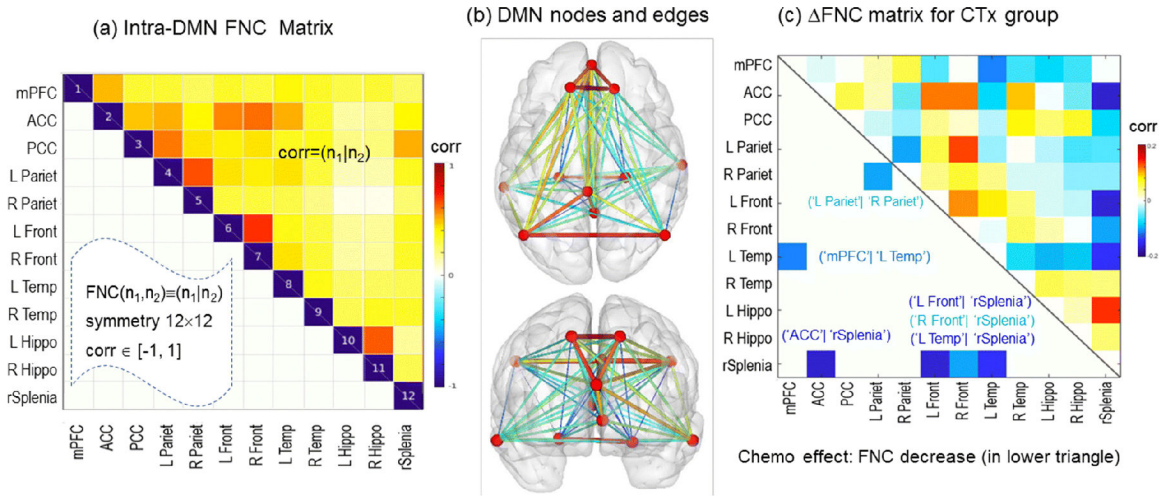

Fig. 1.

Presentation of functional network connectivity (FNC) matrix and FNC data in the CTx group. **(a)** FNC matrix for the meta-level analysis of DMN system. A 12 seed-initiated DMN subnetworks was designated by the anatomical names of each seed region along the x and y axes. Each element in the upper triangle of the symmetrical matrix is color-coded based on the correlation between the indicated subnetworks (corr ∈ [−1,1]). **(b)** Visualization of the nodes and edges of the FNC matrix in MNI standard brain space in the axial and coronal planes. The red nodes represent the 12 seeds and the edges (color-coded linear lines) denote the values of each FNC matrix element values. **(c)** The longitudinal changes of FNC matrix (ΔFNC, in upper triangle) and its significant couplings (in lower triangle) for the CTx group.

Abbreviations: mPFC: medial prefrontal cortex, ACC: anterior cingulate cortex, PCC: posterior cingulate cortex, L Pariet: left parietal cortex, R Pariet: right parietal cortex, L Front: left superior frontal cortex, R Front: right superior frontal cortex, L Temp: left inferior temporal cortex, R Temp: right inferior temporal cortex, L Hippo: left parahippocampal gyrus, R Hippo: right hippocampus gyrus, rSplenia: retrosplenial.

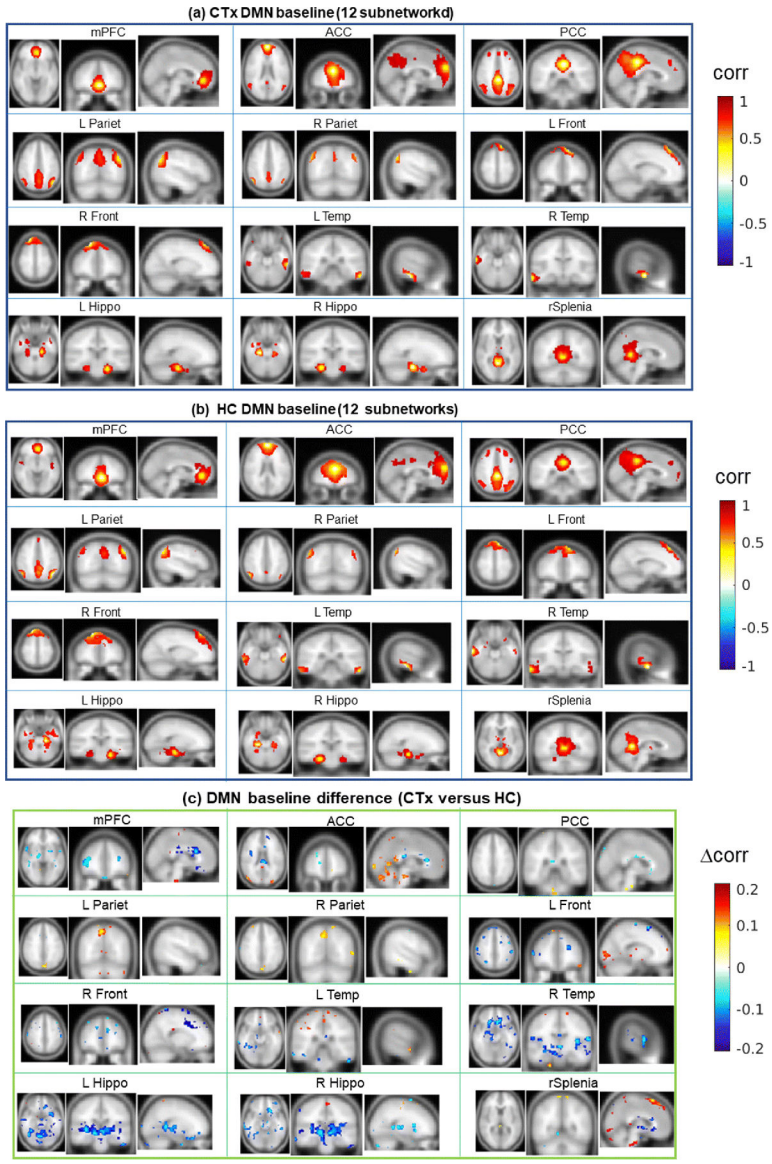

Fig. 2.

The 12 seed-initiated DMN subnetworks at baseline (pre-chemotherapy). **(a, b)** Baseline DMN subnetworks for CTx and HC groups, respectively. **(c)** Baseline differences of DMN subnetworks between the CTx group and the HC group. The DMN subnetworks were constructed from the 12 seeds as functional correlation maps displaying in 12 panels with three orthogonal slices across each of the seeds at (x, y, z) noted in supplemental Table 1. Display thresholding for panel (a) with |corr| > 0.90 and for panels (b) and (c) with |Δcorr |>0.15.

Abbreviations: mPFC: medial prefrontal cortex, ACC: anterior cingulate cortex, PCC: posterior cingulate cortex, L Pariet: left parietal cortex, R Pariet: right parietal cortex, L Front: left superior frontal cortex, R Front: right superior frontal cortex, L Temp: left inferior temporal cortex, R Temp: right inferior temporal cortex, L Hippo: left parahippocampal gyrus, R Hippo: right hippocampus gyrus, rSplenia: retrosplenial.

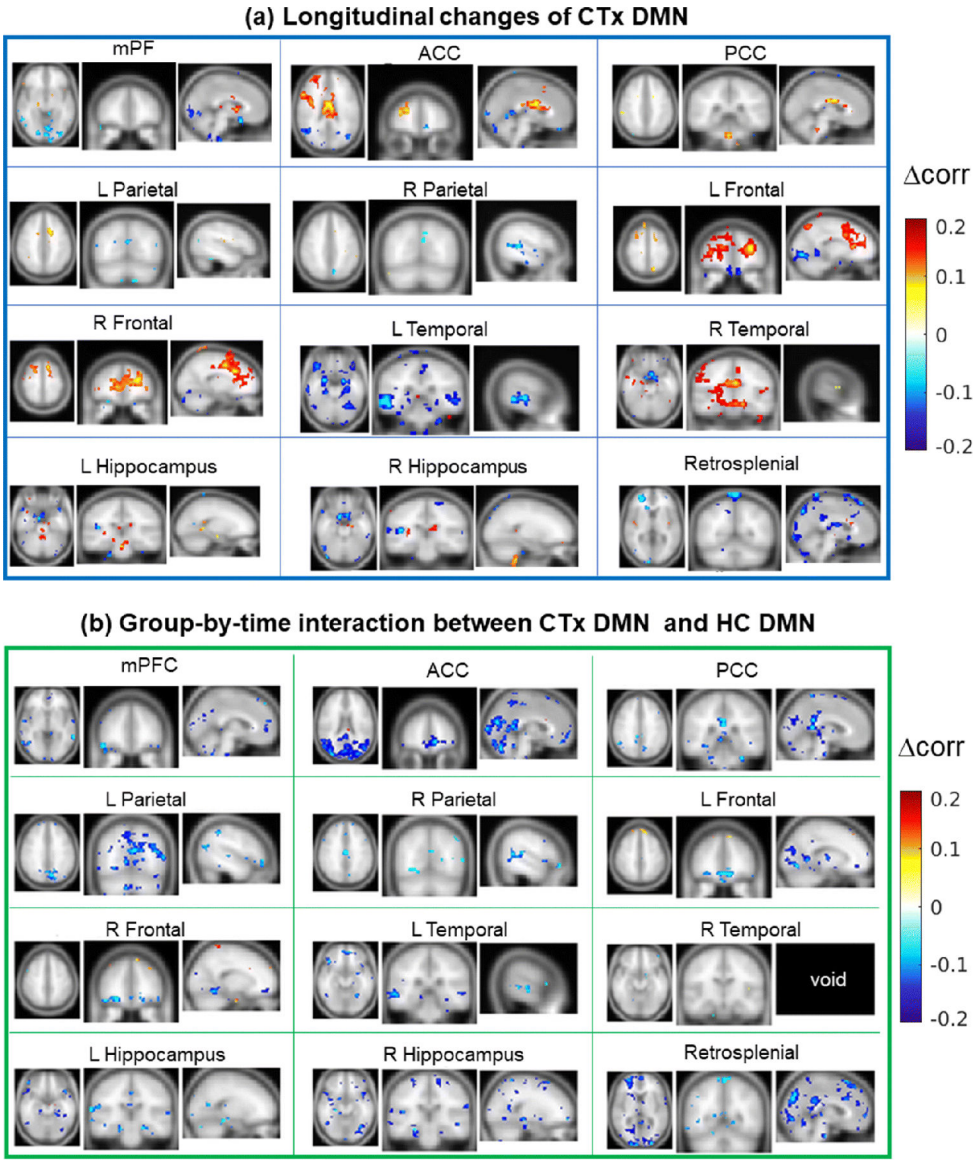

Fig. 3.

Longitudinal alterations of DMN subnetworks. **(a)** Longitudinal changes of DMN subnetworks in the CTx group. **(b)** Group-by-time interaction of longitudinal changes between the CTx group and the HC group. The 12 seed-initiated DMN subnetworks as indicated in supplemental Table 1 were displayed at three orthogonal slices with thresholding |Δcorr|> 0.15.

Void: indicating no group-by-time interaction in the DMN subnetwork initiated at the right temporal cortex.

Abbreviations: mPFC: medial prefrontal cortex, ACC: anterior cingulate cortex, PCC: posterior cingulate cortex, L Pariet: left parietal cortex, R Pariet: right parietal cortex, L Front: left superior frontal cortex, R Front: right superior frontal cortex, L Temp: left inferior

temporal cortex, R Temp: right inferior temporal cortex, L Hippo: left parahippocampal gyrus, R Hippo: right hippocampus gyrus, rSplenia: retrosplenial.

Table 1.

Demographic information and Picture Sequence Memory (psm) testing scores in older women with breast cancer and healthy controls.

	CTx Group (N = 19)	HC group (N = 14)	p-value
Age, years			
Mean (SD)	66.6 (5.24)	68.1 (5.69)	0.32
Range	60–82	60–78	
Race, N (%)			
White	13 (68.4%)	14 (100%)	0.06
Black	6 (31.6%)	0 (0%)	
Cancer Stage, N (%)			
I	7 (36.8%)		Not Applicable
II	9 (47.4%)		
III	3 (15.8%)		
Regimen, N (%)			
TC[a]	10 (52.6%)		Not Applicable
Non-TC[b]	9 (47.4%)		
psm score, Mean ± SD			
Time point 1	111 ±19	101 ± 16	0.1
Time point 2	108 ± 20	108 ± 25	0.98

[a]TC: docetaxel (Taxotere) and cyclophosphamide;

[b]Non-TC, including TCPH: docetaxel (Taxotere), carboplatin, and trastuzumab (Herceptin), ddAC-T: dose dense doxorubicin (Adriamycin) and cyclophosphamide, followed by paclitaxel (Taxol); TAC: docetaxel (Taxotere), doxorubicin (Adriamycin), and cyclophosphamide; Paclitaxel/trastuzumab; Carboplatin/paclitaxel.

TP: time point. psm: Picture Sequence Memory.

Table 2.

Significant couplings from the meta-level functional connectivity network (FNC) analysis for the chemotherapy (CTx) group and the healthy control (HC) group ($p_{FDR}<0.05$).

1. Baseline FNC difference: FNC(CTx) vs. FNC(HC)		
Coupling	**Δ*corr***	***t-test* (tvalue±sd [CI_{low},CI_{high}])**
(‘ACC’|‘L Temp’)	0.11	2.30±0.14 [0.03,0.29]
(‘ACC’|‘rSplenia’)	0.12	2.29±0.10 [0.03,0.22]
(‘R Temp’|‘R Hippo’)	−0.13	−2.44±0.12 [−0.25,−0.03]
(‘L Hippo’|‘rSplenia’)	−0.20	−2.94±015 [−0.35,−0.07]
2. FNC change for the CTx group: ΔFNC(CTx)		
Coupling	**Δ*corr***	***t-test* (tvalue±sd [CI_{low},CI_{high}])**
(‘mPFC’|‘L Temp’)	−0.11	−2.06±0.11 [−0.20,−0.08]
(‘L Pariet’|‘R Pariet’)	−0.10	−2.05±0.10 [−0.20,−0.07]
(‘ACC’|‘rSplenia’)	−0.14	−2.44±0.12 [−0.27,−0.10]
(‘L Front’|‘rSplenia’)	−0.16	−2.56±0.13 [−0.28,−0.10]
(‘R Front’|‘rSplenia’)	−0.12	−2.24±0.11 [−0.23,−0.11]
(‘L Temp’|‘rSplenia’)	−0.17	−2.54±0.14 [−0.30,−0.12]
3. FNC change for the HC group: ΔFNC(HC		
None		
4. Group-by-time Interaction: ΔFNC(CTx) vs. ΔFNC(HC)		
Coupling	**Δ*corr***	***t-test* (tvalue±sd [CI_{low},CI_{high}])**
(‘mPFC’|‘ACC’)	−0.11	−2.11±0.10 [−0.32,−0.03]
(‘mPFC’|‘L Front’)	−0.15	−2.47±0.11 [−0.28,−0.08]
(‘mPFC’|‘L Temp’)	−0.20	−2.47±0.14 [−0.36,−0.10]
(‘ACC’|‘rSplenia’)	−0.18	−2.45±0.14 [−0.32,−0.09]
(‘L Pariet’|‘L Hippo’)	−0.13	−2.04±0.12 [−0.26,−0.02]
(‘L Pariet’|‘R Hippo’)	−0.16	−2.07±0.15 [−0.32,−0.05]
(‘L Pariet’|‘rSplenia’)	−0.17	−2.13±0.15 [−0.33,−0.04]
(‘L Temp’|‘rSplenia’)	−0.19	−2.30±0.16 [−0.36,−0.08]

Abbreviations: CTx: chemotherapy group; HC: health control group; FDR: false discovery rate; corr: correlation coefficient (Pearson); t score: statistical t-test value; FNC: functional network connectivity;

ΔFNC: longitudinal FNC change; Δtcorr: coupling strength change (or difference); tvalue, statistical t-test value; [CI_{low}_CI_{high}], 95% confidence interval.

mPFC: medial prefrontal cortex, ACC: anterior cingulate cortex, PCC: posterior cingulate cortex, L Pariet: left parietal cortex, R Pariet: right parietal cortex, L Front: left superior frontal cortex, R Front: right superior frontal cortex, L Temp: left inferior temporal cortex, R Temp: right inferior temporal cortex, L Hippo: left parahippocampal gyrus, R Hippo: right hippocampus gyrus, rSplenia: retrosplenial.